Estimating Localization of Various Statins within a POPC Bilayer

Jacob Olondo Kuba[1,‖], Yalun Yu[2,‖], and Jeffery B. Klauda[1,2*]

[1]Department of Chemical and Biomolecular Engineering, [2]Biophysics Graduate Program,
University of Maryland,
College Park, MD 20742, USA

*Corresponding Author: jbklauda@umd.edu
‖Equal Contribution

Abstract

As a class of drugs prescribed to heart disease patients, statins are among the most popular prescription drugs in the world. Over the years, statins have been shown to have beneficial effects on patients via pathways independent of their effect on cholesterol. These pleiotropic effects vary across the different statins, and a growing hypothesis is that they are related to the localization of the statins in and their effect on the membrane. In this study, we use molecular dynamics (MD) simulations with the all-atom force field (CHARMM36) to investigate the localization of statins (atorvastatin, cerivastatin, lovastatin, and pravastatin) in a POPC bilayer and how they affect the acyl chain order parameters (S_{CD}), surface area per lipid (APL), and thicknesses of the bilayer. The data obtained from 500 ns simulations suggests that lovastatin is localized deepest in the membrane, mostly interacting with the hydrophobic core, cerivastatin is slightly closer to the bilayer/solvent interface than lovastatin and interacts with the headgroups via its dihydroxy acid group, and pravastatin is found closest to the bilayer/solvent interface, its hydrophobic rings interacting mostly with the region around the acyl's carbonyl and its dihydroxy acid interacting with the solvent and the headgroups. Consistent binding of atorvastatin to the bilayer is not observed during our simulation. The statins differentially decrease the S_{CD} and APL and most of the bilayer thicknesses, but these effects are modest. Overall, as expected, the localization of statins seems to follow their hydrophilicity, and given previous data showing the relationship between statins hydrophobicity and pleiotropic effects, one would expect statins that localize and interact with different regions of the membrane to have different effects. This research provides some important insight to statin localization in a simplified model of a cellular membrane.

1. Introduction

Cardiovascular disease, particularly coronary heart disease (CHD), has been the leading cause of death in developed countries for many years[1]. It is no surprise that statins, a class of powerful cholesterol-lowering drugs, are among the most prescribed drugs in the world[2] given the high number of people affected by CHD and the strong correlation between cholesterol and CHD[3-6]. Statins inhibit 3-hydroxy-3-methylglutarylcoenzyme A (HMG-CoA) reductase, which catalyzes the reduction of HMG-CoA to mevalonate, the rate-limiting reaction in cholesterol biosynthesis[7]. Multiple large secondary and primary intervention trials have demonstrated the efficacy of statins in reducing CHD morbidity and mortality[8]. Interestingly, the positive impact of statins on CHD patients observed in numerous clinical trials appears to be greater than what would be expected from a decrease in serum cholesterol only[9]. Statins have been shown to have many effects independent of their cholesterol-lowering effect, and these cholesterol-independent or 'pleiotropic' effects include restoration of endothelial function, decrease in oxidative stress, a decrease of inflammation and many more[9-13].

Although statins share the important dihydroxy acid group, as shown in Fig. 1, they have subtle differences in their chemical structure that result in differences in pharmacokinetics, dynamic action, pleiotropic, and adverse effects among them[14-17]. There is emerging evidence supporting the notion that the amphiphilicity of statins impacts the gravity of certain adverse effects[17]. In fact, the statin cerivastatin had to be removed from the market in 2001 due to its strong link with unacceptable rates of rhabdomyolysis (1/316,000) compared with pravastatin (1/27.1 million) and other statins in its class, causing 51 fatalities worldwide[18]. An established hypothesis proposes that the localization of statins in the cellular membranes determines or is associated with their biological properties[16, 19, 20]. However, understanding of the relationship between statin localization and pleotropic remains unclear. The difficulty of studying and visualizing drug-membrane interactions in tissues is one of the main barriers to gaining a better understanding. Nevertheless, membrane models have been used in a few studies to study the interaction of statins with membranes. However, additional studies are still needed to explore in more details the different aspects of the drug-membrane interactions, notably the localization of the drugs in the membrane and their effects on the physical properties of the membrane.

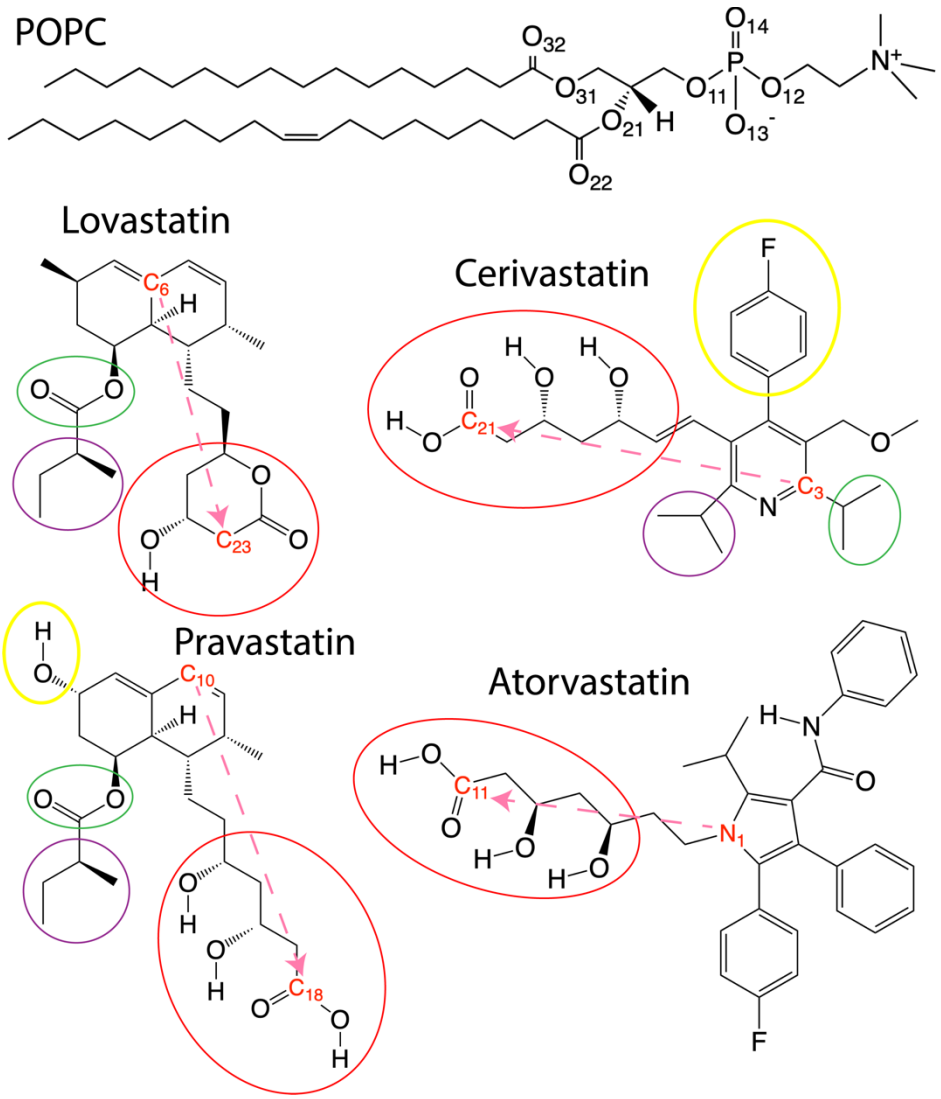

Fig. 1. Chemical structures of compounds studied, 1-palmitoyl-2-oleoyl-sn-glycero-3-phosphocholine (POPC), cerivastatin (CER), atorvastatin (ATO), lovastatin (LOV), and pravastatin (PRA). Arrows in pink with atom names in red font on both ends are the directors used in the orientation analysis. On CER, ATO, and PRA, the atoms in the red ellipse is the dihydroxy pentanoate group (DHP). On LOV and PRA, the atoms found in the green and purple ellipses make up the ester group (ROOR) and the 1-methylpropyl group (1MP), respectively. On LOV the red ellipse marks the lactone group (LAC). The yellow ellipse on CER marks the fluorophenyl (FPH), and the one on PRA marks the hydroxyl group (ROH). The purple ellipse on CER marks the proximal isopropyl group (PIP), and the green one marks the distal isopropyl (DIP). The non-highlighted atoms for all the molecules are arbitrarily called the main hydrophobic moiety (MHM).

The interaction of statins with bilayer phospholipids is expected to be heavily affected by the amphiphilicity of each statin. Galiullina et al. used solid-state NMR spectroscopy to study the interaction of six different statins, four of which are investigated in this paper, with large 1-palmitoyl-2-oleoyl-sn-glycero-3-phosphocholine (POPC) unilamellar vesicles[21]. Galiullina and colleagues showed that the hydrophobic statin cerivastatin binds to the membrane more deeply, primarily interacting with POPC via carbons on the acyl chain just below the glycerol backbone, than the lesser hydrophobic statin atorvastatin that primarily interacts with glycerol backbone[21]. Their work also showed that the very hydrophilic pravastatin binds to the membrane less frequently than the other statins[21], and this is in accordance with previous experimental work demonstrating that pravastatin relies on active transport to cross the membrane[22]. Galiullina and colleagues showed the localization of two additional statins, fluvastatin and rosuvastatin, but unfortunately, some hydrogen NMR resonance lines of the statins were overlapping with the POPC signal, making it difficult to determine the location of lovastatin and pravastatin[21]. Galiullina and colleagues also showed that statins lower the acyl-chain deuterium order parameters (S_{CD}) of POPC lipids in unilamellar vesicles, with each statin exerting subtly different effects[21]. From the same research group, Shurshalova et al. recently published a paper in which they demonstrated that lovastatin is mostly associated with the hydrocarbon tails of dodecylphosphocholine (DPC) and sodium dodecyl sulfate (SDS) micelles, using NMR spectroscopy and coarse-grained molecular dynamics (MD) simulations[23].

The computational work by Shurshalova et al. provided insight into the positioning of lovastatin in micelles. Nevertheless, their approach has two main limitations that we aim to address, namely the use of micelles as models for the membrane and the use of coarse-grained force fields. Although micelles can be a good model for biological membranes, their surface has much higher curvature than that of biological membranes[24]. The high surface curvature of micelles can influence the interactions between the statins and phospholipids. MD simulations with coarse-grained force fields have been useful in the study of biological membranes[25]. However, coarse-grained force fields are not as accurate in comparison to their atomistic counterparts[26] and cannot provide certain details, such as atomistic details[25, 26]. For example, the order parameters for individual carbons can be calculated directly using all-atom FFs, while with coarse-grained force fields one only gets an estimation of the average based on chain direction.

Our work aims to use atomistic MD simulations to study the interactions of four statins molecules with a nearly flat POPC bilayer to provide more insight into the localization of each statin in the membrane and the effects of statins on physical properties of the membrane. MD simulations are useful in providing certain relevant details that are experimentally inaccessible or costly in both time and money[27]. MD simulations with atomistic resolution are an excellent tool for supplementing experimental techniques that have limited resolution, especially when studying interactions of drugs with biomolecules where insight into the interaction of single atoms can be extremely important. For example, the NMR study by Galiulinna et al. could not localize lovastatin and pravastatin due to lack of resolution in the NMR data[21]. This work aims to accurately find the location of these two drugs, along with atorvastatin and cerivastatin, in the POPC bilayer. We also aim to determine their effects on physical characteristics of the bilayer, namely, the area per lipid, the chain order parameters, and the thickness. Although MD simulations have been a great tool in the study of many biological systems, there are still limitations, such as the force field accuracy and time scale limitation due to computational limitations[24, 28]. Simulations at the sub-μs time scale may not be long enough to allow the statins to reach their thermodynamically equilibrated state of partitioning between the statins in solution and those that bound to the membrane. However, 500 ns may be long enough to study the localization in the membrane as long as there are some statins diffusing into the membrane. Another important limitation that applies to both the MD simulation and the NMR studies is the use of simplistic membrane models that lack all the other lipid and protein components of the cellular membranes that may play a role. For instance, as highlighted earlier, the movement of pravastatin across the membrane depends on transporter protein[22], which is an example to highlight the limitation of the simplistic membrane models used in these studies. Nevertheless, membrane models have been a great tool for increasing the understanding of many drugs despite their limitations[27]. The goal of this study is to gain more knowledge on the interaction of statins with membranes as that may play an important role in the different pleiotropic effects of the different statins.

2 Methods

2.1. System setup and simulation protocol

Systems of pure POPC and POPC with atorvastatin, cerivastatin, lovastatin, and pravastatin were simulated for 500 ns at a physiological temperature of 37 ºC. All the systems had 40 lipids per

leaflet and 120 water molecules per lipid, bringing the totals to 80 POPC and 9600 water molecules. The large number of water molecules is needed for the full hydration of the statin molecules. The use of only 40 lipids per leaflet is motivated by the desire to minimize the size of systems given the large amount of water per lipid required to fully hydrate the statins. A smaller system size is less computationally demanding given the high number of total systems being simulated. Test systems made up of pure phospholipids at similar leaflet size behaved normally, reinforcing the position that smaller systems could be appropriate for such simulations. The POPC bilayer was generated in rectangular boxes and a tetragonal cell ($x = y \neq z$) using CHARMM-GUI *Membrane Builder* and equilibrated using the standard six-step process in NAMD[29-32]. The statin molecules were built using the CHARMM-GUI *LigandReader & Modeler* tool[29-33] and modeled using the CHARMM General FF[34-38]. The provided stream file and penalty scores are included in the supporting document.

In order to replicate the 20 mol% of statins used by Galiullina et al,[21] twenty molecules of each of the four statins were randomly positioned in their respective system with a minimum distance of 15 Å away from the POPC bilayer, ten molecules on each side of the bilayer. The statins were directly added to the POPC bilayers built from CHARMM-GUI using the CHARMM[39] software (version c41b2) and then equilibrated in NAMD using the standard six-step process provided by CHARMM-GUI. Atorvastatin, cerivastatin, and pravastatin molecules were added in their deprotonated dihydroxy heptanoate form with positive counterions, Ca^{2+} for atorvastatin and Na^{+} for cerivastatin and pravastatin. The statin-cation salt combinations were chosen to match the experiment, and they match the form in which they are most prescribed. Lovastatin was added in its lactone ring form. The initial dimensions of all the systems were 60 × 60 × 160 Å. Each system was replicated to have three replicas per drug. In addition to the 20 mol% concentration simulations, 3 replicas of 400-ns-long titration simulation were run for each statin to study the effect of self-aggregation of the statins. These systems contain the same number of lipids and water molecules and were built in the same way as their high concentration counterparts. The only difference is that they contain only one statin molecule per system.

The CHARMM36 lipid force field[40] was used with the TIP3P water model[41, 42]. The simulations were carried out using the NPT ensemble with a constant number of molecules at constant pressure of 1.01325 bar and constant temperature of 310.15 K in NAMD[32]. The

temperature was kept constant through Langevin dynamics with a damping constant of 1.0 ps^{-1}, and the pressure was kept constant through the Nosé-Hoover Langevin-piston[43, 44]. Van der Waals interactions were estimated using Lennard-Jones potential with a force-switching function[45] over the range of 10 to 12 Å. Long-range electrostatic interactions were modeled using the particle-mesh Ewald (PME) method. Long-range electrostatic interactions were calculated every step using a sixth-order interpolation and direct spacing tolerance of 10^{-6}. Bond lengths involving hydrogen were kept constant by the RATTLE algorithm[46]. The time step for all the simulations was 2 fs, and the coordinates were saved every 5 ps. Visual Molecular Dynamics (VMD)[47] was used to calculate the chain order parameters, observe the behavior of statin molecules throughout the simulation, and to obtain snapshots.

Given the desire to capture the interactions of statins with phospholipid bilayer without bias, statins were placed in solution at a distance from the membrane to allow them to freely diffuse to the membrane. Since the statins' interactions with the membrane are dependent on the pseudo-random diffusion of statins toward the membrane, three systems were built for each statin drug, and the statins had different spatial configurations in the simulation box for each system. To minimize the water aggregation of statins given their moderate to high lipid partitioning index[21], the statins were placed in such a way to maximize the intermolecular distance.

2.2 Analysis

The focus of this work is on systems in which at least one statin molecule bound to the membrane since our main objective is the localization of the statins within the membrane. We chose to focus on systems where the statins showed binding, which is at least partial integration into the membrane to remove the ambiguity in establishing what would be considered as a close enough interaction. The main analyses shown in this work are the electron density profiles (EDP) since they contain information about the localization of the statins in the membrane. Additionally, area per lipid (APL), chain order parameters (S_{CD}), center of mass (COM) position of statin, tilt angle, and radial distribution functions (RDFs) are also presented here.

The overall APL is calculated by dividing the total area occupied by the bilayer by the number of lipids in the bilayer. The S_{CD} was calculated using VMD. S_{CD} was calculated by the formula:

$$S_{CD} = \left|\langle \frac{3}{2}\theta \ - \frac{1}{2}\rangle\right| \qquad (1)$$

where θ is the angle between the C-H vector and the bilayer normal. The S_{CD} is calculated by averaging all the C-H vectors of each carbon in the bilayer throughout the last 300 ns of the simulations.

As for EDP calculations, the bilayer was first recentered in the simulation box in such a way that the center of the bilayer is positioned at z=0 Å. The EDP of each atom was calculated, and the atoms' EDPs were combined to form the EDP of their respective molecules. EDPs were calculated along the z-axis with a 0.2 Å slab thickness. EDPs were also used to calculate the overall bilayer thickness (D_B), headgroup-to-headgroup distance (D_{HH}), and hydrophobic core thickness ($2D_C$). D_B represents the distance between the half-maximums of the water EDP. D_{HH} is defined as the distance between the peaks of the total EDP, and $2D_C$ is the distance between half-maximums of the acyl chains EDPs excluding the carbonyl group. The errors were obtained from block averages for all the calculations.

The determination of the statins' orientation in the bilayer consisted of calculating the angle made by the statin vectors defined in Fig. 1 with the bilayer's normal. The vectors were chosen by looking at the rough polarity in hydrophobicity of the statins, that is, going from the very hydrophobic cyclic hydrocarbon to the very hydrophilic negatively charged deprotonated carboxylic acid (in the case of lovastatin, the lactone group).

3. Results

3.1 Simulations of Statin Binding

For each drug, three replicas were simulated for both the 20 mol% system and the titration system. The z coordinates of the drug molecules during the simulations can be found in Fig. S1. All the 20 mol% systems showed close (less than 5 Å) and transient interactions between the statin molecules and the surface of the bilayer less than 10 ns after the start of the simulation. However, as the simulations progressed, the differences between the statins became more apparent as the drug-drug and drug-lipid interactions increasingly differed across the different drugs. For instance, clusters of five or more molecules in solution started forming in lovastatin and cerivastatin systems as early as 20 ns into the simulation. Atorvastatin displayed a similar behavior with the formation

of clusters early in the simulation. The significant increase of the short-range COM RDFs for atorvastatin and cerivastatin (Fig. S2) indicates strong self-aggregations. Pravastatin behaved very differently and had much less cluster formation, which is demonstrated by the steady COM RDFs during the entire simulations. Thus, pravastatin molecules had more freedom in their diffusion in the solution in comparison to the other statins.

Because the D_{HH} of POPC bilayer is about 40 Å, steady positionings of the statin molecules within the range of -20 Å to 20 Å (Fig. S1-a) were identified as "binding" events. In the 20 mol% simulations, membrane binding happened in two out of the three pravastatin systems but not in any of the atorvastatin systems, despite the close interactions between the headgroup of the bilayer and the carboxylate group of a few statin residues. Two out of the three cerivastatin systems and one out of the three lovastatin systems had at least one statin residue bind to the bilayer at the end of the simulation. The drugs' transition from the solution to the inside of the bilayer happened in the first 150 ns for most systems. However, one cerivastatin system was an exception because the statin did not bind to the bilayer until 308 ns. One pravastatin system had two molecules bind to the membrane (Fig. 2), while the other pravastatin system only had one. Interestingly, the only lovastatin system showing binding had three lovastatin molecules deep in the bilayer (Fig. 2). One of the two cerivastatin systems with one residue in the bilayer is also shown in Fig. 2 along with an atorvastatin system with close interactions of statins and the membrane, albeit without binding. The reason for no atorvastatin binding is its high tendency of self-aggregation preventing the free diffusion of single atorvastatin into the membrane. This self-aggregation was ruled out in the titration simulations, where atorvastatin bound to the membrane in all the three replicas at an early stage (Fig. S1-a). If not mentioned specifically, the analyses in the rest of the paper are based on the systems shown in Fig. 2 since the focus here is location of the binding statins and their influence on the membrane structure. Table S1 summarizes how many statin molecules bound to the membrane for each replica of the three statin systems, and the time binding happened for each individual molecule. The specific pravastatin system was chosen because it had the greatest number of statins in the membrane (PRA replica 3 in Table S1). The specific cerivastatin system (CER replica 3 in Table S1) was chosen over the other ones because of the early binding of the statin into the membrane. The lovastatin system (LOV replica 2 in Table S1) was chosen because it was the only one out of the three with binding. The specific atorvastatin system (ATO replica 1 in Table S1) was chosen because it had more transient interactions with the membrane in

comparison to the other atorvastatin systems. The goal of this work is to study the interactions of statin with the membrane and the subsequent effect on the membrane. For this reason, we chose to focus on replicas where the most binding occurred to investigate in detail the localization and orientation within the membrane of the statins in question.

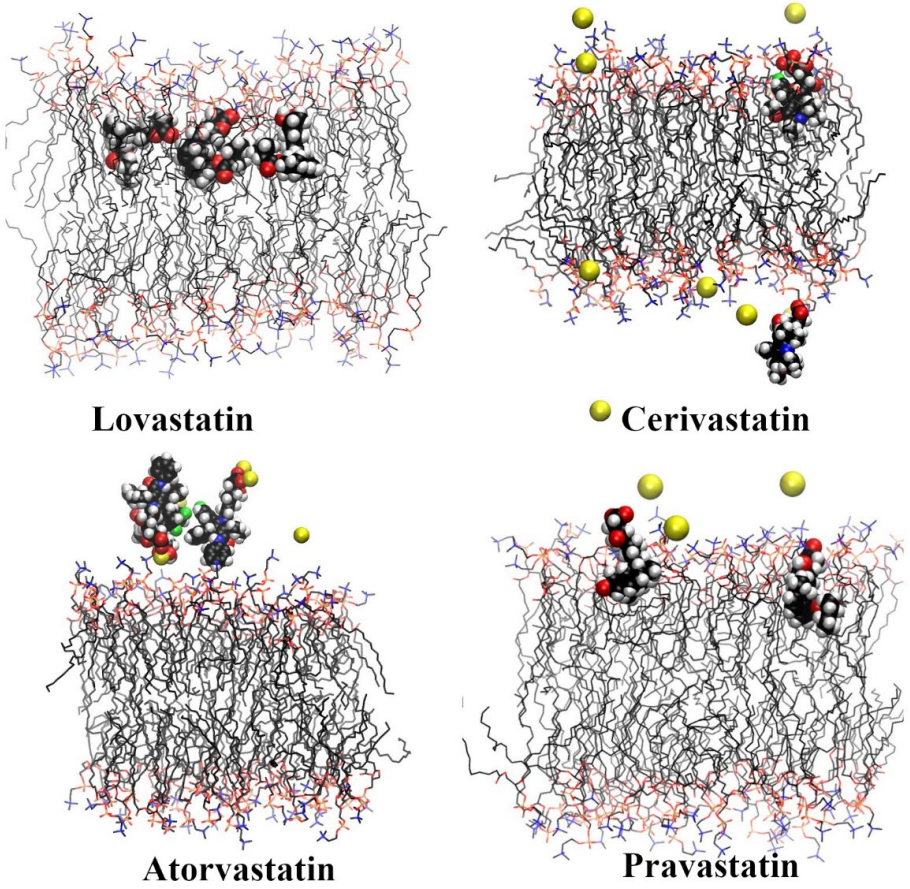

Fig. 2. Capture of statins in the last nanosecond of the simulation. Only statins in contact with the bilayer are shown. The yellow atoms represent the positive metal ions, calcium for atorvastatin, and sodium for pravastatin and cerivastatin. C in black, H in white, O in red, N in blue, F in green, and P in orange.

3.2 Surface Area per Lipid (APL)

The APL provides an estimate of the lateral packing of the membrane[24]. The APL can serve as a means of comparison between MD simulations and experiments. Finally, the APL plays an important role in MD simulations as it is used to monitor the time at which the system reaches equilibrium. Knowing the time at which the system reaches equilibrium is critical in the analysis

of data because most of the analysis is done with the data obtained after equilibrium. Thus, the equilibrium points were detected using the pymbar package[48] with the entire simulation as input if there is no drug binding but only part of the simulation after binding if there is a binding event. The APLs as a function of time are found in Fig. S4 with the detected starting times of equilibrium. The average APLs based on the equilibrium parts, which are reported in Table 1, followed a trend where the number of statin molecules embedded into the bilayer positively affected the APL values. The pure POPC system had an APL of 65.23 ± 0.03 Å^2. The lovastatin and pravastatin systems had the highest APL, 68.04 ± 0.03 Å^2 and 67.28 ± 0.03 Å^2, respectively. The higher APL observed in the lovastatin system in comparison to that of the pravastatin is in part due to the higher number of statins penetrating the membrane, three for lovastatin versus only two for pravastatin. The cerivastatin system, which had only one statin molecule bind to the bilayer, had an APL of 66.82 ± 0.03 Å^2, a value lower than the lovastatin and pravastatin systems but higher than the 65.45 ± 0.03 Å^2 of the atorvastatin system that showed no incorporation of statin molecules into the bilayer. The atorvastatin system caused a very small decrease in APL.

Table 1: Surface area per lipid (APL) for POPC-pure, PRA, LOV, CER, and ATO systems.

System	APL (Å^2) ± standard error
POPC pure	65.71 ± 0.03
PRA	67.28 ± 0.03
LOV	68.04 ± 0.03
CER	66.82 ± 0.03
ATO	65.45 ± 0.03

3.3 Acyl Chain Order Parameters (S_{CD})

S_{CD} measures the overall order of the lipid bilayer and provides information on the specific conformations adopted by the atoms within the lipid tail. S_{CD} can be measured with NMR as the average orientation of the carbon-deuterium vectors with respect to the magnetic field, which is generally set to be parallel to the membrane's normal. MD simulations utilizing an all-atom force

field can easily and directly estimate S_{CD} by averaging the orientation of the C-H bond vector with respect to the bilayer normal assuming the C-D bond orientation in experiment is identical to the C-H bond in our simulations. Chain order increases as the S_{CD} value increases, with a perfectly ordered chain in the all-trans configuration reaching 0.5 S_{CD} values.

To observe the effect of the statins on the order parameter, S_{CD} of each leaflet was calculated separately during the time window of drug binding. POPC has a fatty acyl chain attached to carbon 2 and 3 of the glycerol backbone (Fig. 1). Overall, as expected, the order decreased gradually from the eighth to the last carbon of the fully saturated palmitoyl or the *sn*-1 fatty acyl chain. For the palmitoyl chain, differences between the pure POPC and the statin systems were observed, especially from the fourth to the fourteenth carbon (Fig. 3). The lovastatin and pravastatin systems were the least ordered and most different from the pure POPC system. Interestingly, the binding drugs affected the S_{CD} of the opposite leaflet more than the leaflet it resided. Fig. S5 compares the palmitoyl chain of the "opposite" leaflet for the four drugs directly and Table 2 lists the difference between the S_{CD} of pure POPC and each POPC-Statin system. The lovastatin system had the lowest S_{CD} followed by pravastatin, cerivastatin, and atorvastatin, respectively. This means the lowering effect on the "opposite" leaflet is positively correlated with the number of binding drug molecules (see Table S1), which can be explained by the expansion of the bilayer in the *x*-*y* plane and the fact that order parameters are inversely correlated with APL[49]. Since the drug molecule(s) took up space in the leaflet it bound to, the change in the actual APL was less pronounced, thus smaller changes in S_{CD} were observed. In the case of lovastatin (replica 1), the binding drugs showed an ordering effect on the top six carbons. This ordering effect is consistent with the influence of sterols on chain order parameters[50] considering the ring structures they share, and it is also consistent with the deeper penetration and the larger number of drug molecules bound to the bilayer compared to lovastatin and pravastatin. The fatty acyl attached to carbon 2, oleoyl, or the *sn*-2 chain, is generally more disordered given the cis double bond between carbon 9 and carbon 10 (Fig. 1). The *sn*-2 chain showed very little variation in order parameters between the pure POPC and the statin systems (Fig. S6), though the pravastatin system displayed slightly more disorder from the eleventh to the seventeenth carbon.

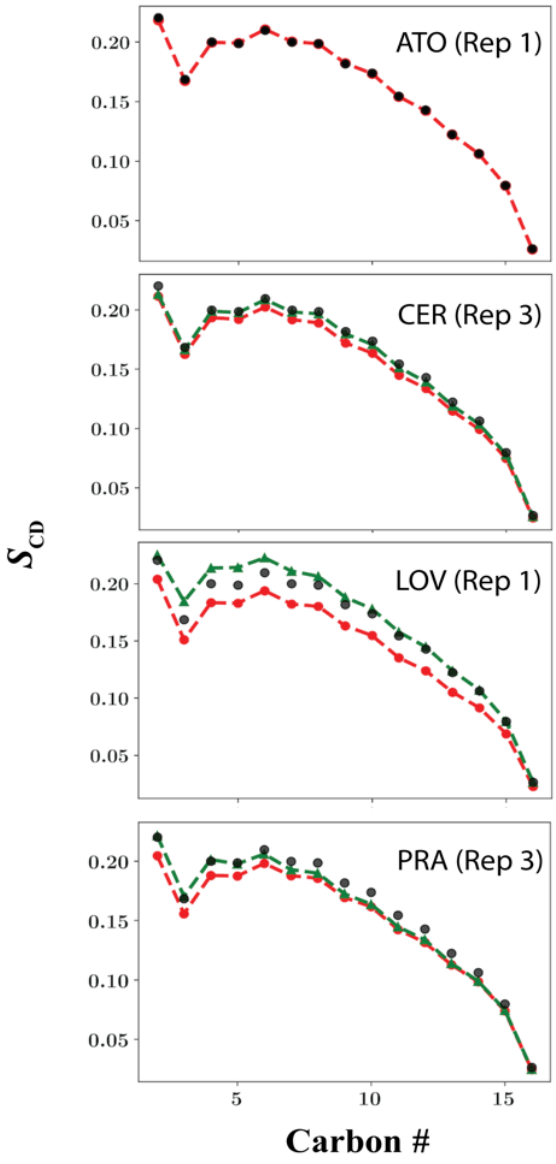

Fig. 3. S_{CD} as a function of chain carbon number for the palmitoyl (*sn*-1) chains in statin systems compared to pure POPC. Black dots: pure POPC; green triangles with dashed lines: the drug-binding leaflet; read dots with dashed lines: the other leaflet. For ATO, the last 300 ns is used; for the other three systems, the time window of drug binding is used. Standard errors are smaller than the symbol sizes and not shown.

Table 2. Averaged difference in order parameter values between *sn*-1 carbons of the pure POPC and POPC-statin systems on the key carbon range (C4:C12).

statin	LOV	PRA	CER	ATO
Difference	0.018	0.012	0.08	0.06

3.4 Electron Density Profiles (EDPs) and Bilayer Thickness

EDPs provide insight into the spatial distribution of atoms along the *z* axis of the simulation box, and it is a great tool for the localization of molecules in and around the membrane. Cerivastatin, lovastatin, and pravastatin had at least one out of their three systems show penetration of at least one statin molecule into the bilayer. Given the fluid nature of lipid bilayers, all the three statins interacted with all regions of the leaflet, i.e., the phosphatidylcholine, glycerol backbone, and acyl chains. However, the interaction with POPC is varied across the three statins as each appears to have a particular positional distribution curve (PDC) (Fig. 4). Statins are amphipathic compounds, and we predicted that they would orient themselves in ways that maximize hydrophilic interactions with the polar headgroups and solvent and the hydrophobic interactions with the core of the membrane. We took advantage of the all-atom force field to obtain atomistic resolution for the interactions of the statins and POPC. We divided each statin in atom groups to see where in the membrane and with which POPC's atoms the group localize and interact with the most. Fig. 1 shows how we subdivided the statins.

Pravastatin's PDC within the membrane peaks at z = 14.5 Å (Fig. 4), which is very close to the peak location of carbonyl at 14.7 Å (Table S2). Pravastatin's PDC can almost be superimposed onto that of the carbonyl of the lipid (Fig. 4). Pravastatin's PDC is also close to that of the glycerol backbone although the latter is slightly shifted to the right with its peak occurring at z = 15.5 Å (Table S2). The main hydrophobic moiety (MHM), peaking at 14.1 Å (Fig. S7C and Table S3), interacted mostly with the carbonyl, the glycerol, the upper region of the acyl near the carbonyl (Fig. S7C). The EDPs show that the 1-methylpropyl group (1MP), peaking at 12.9 Å, attached to the ester group (ROOR) was localized deeper in the bilayer than the rest of the molecule (Fig. S7C and Table S2). The EDPs show that ROOR and the hydroxyl group (ROH) had similar localization in the bilayer as both had broad overlapping curves (Fig. S7C). ROH and ROOR peak at 14.9 and 14.3 Å, respectively, indicating a high degree of freedom of motion that is, however,

centered around the carbonyl of POPC (Fig S7C and Table S3). The dihydroxy pentanoate group (DHP), the active site binding part of the molecule, is very hydrophilic, and unsurprisingly, the EDP shows that this group was localized much closer to the headgroup than the rest of the molecule with the PDC's peak occurring at z = 19.9 Å, right in the middle of the phosphate and choline peaks (Fig. S7 and Table S3).

Like pravastatin, EDPs show that cerivastatin maintained a certain orientation while interacting with the POPC bilayer. The peak of CER's PDC molecule is located at z = 11.9 Å which corresponds to the region mostly occupied by atoms just below the carbonyl (Fig. 4). PDC of cerivastatin ranges from the middle upper acyl region to the phosphatidylcholine (PC) region (Fig. 4). As for the different CER's parts, the PDC of DHP is closer to the bilayer surface than the rest of the molecule and peaks at z = 17.9 Å (Fig. S7A and Table S3). The PDCs of the glycerol, the phosphate, and choline atoms peak at z = 15.7 Å, z = 19.3 Å, and z = 20.5 Å, respectively (Fig. S7A and Table S3). PDH's 17.9 Å peak is just 1 Å less than the glycerol, and PC atoms peaks. Moreover, there is a great overlap between the dihydroxy pentanoate (DHP) PDC and the PC's PDC (Fig. S7A). Cerivastatin has a phenyl with fluorine attached para to the rest of the molecule (Fig. 1). The PDC of the fluorophenyl group (FPH) peaks at z = 13.5 Å and greatly overlaps with both the CH2 and glycerol distribution curves (Fig. S7A and Table S3). However, the FPH peak is 1.4 Å closer to the bilayer center than the carbonyl's peak, which occurs at z = 14.9 Å (Fig. S7A and Tables S2 and S3). Cerivastatin has two isopropyl groups attached to the main ring (Fig. 1). One isopropyl group is para or distal (DIP) to DHP, and the other is ortho or proximal (PIP) to DHP. The EDPs show that the two IP groups were localized in different regions of the bilayer with the PIP's PDC peaking at z = 11.9 Å in comparison to 8.3 Å for DIP (Fig. S7A and Table S3). In fact, the PDC of DIP and that of the atoms making up the *cis* double bond in the oleyl chain (CH) of POPC (Fig. 1) strongly overlap. However, the CH's PDC is slightly shifted toward the center of the bilayer by less than 1 Å, peaking at z = 7.5 Å (Fig. S7A and Table S2). The main pyridine ring attached to the ether, making up the MHM, had a positional distribution like that of DIP and FPH combined, with its maximum located at z = 11.3 Å (Fig. S7A and Table S3). The EDPs show the MHM group localized within the acyl chain while interacting with the carbonyl and glycerol occasionally.

Unlike pravastatin and cerivastatin, lovastatin lacks the polar dihydroxy pentanoate (DHP) (Fig. 1), the EDPs also show this reduced hydrophilicity. The PDC of lovastatin peaked at z = 10.9

Å (Fig. 4), well within the CH2 curve of the bilayer (Fig. 4), indicating that lovastatin spent a considerable amount of time in the acyl chain region of the bilayer. Moreover, the PDCs of the carbonyl and glycerol peak at 14.9 Å and 15.9 Å (Fig. S7 and Table S3), respectively, well above the 10.9 Å of lovastatin and further indicating that lovastatin heavily interacted with the acyl chains. Unlike pravastatin and cerivastatin, the PDCs of lovastatin's components are very broad and show a high degree of overlap with one another (Fig. S7B). Lovastatin has a lactone ring (LAC) instead of DHP found in the other statins (Fig. 1). LAC's PDC is broad with no peak but a flat top (Fig. S7B). This flat "peak" is maintained from z = 11 Å to z = 14 Å (Fig. S7B), suggesting a high degree of freedom of motion. However, the maximum for the lactone distribution occurred at z = 11.9 Å, one Å closer to the bilayer's surface than the overall molecule (Table S3). Lovastatin also has an ester group (ROOR), and its PDC is nearly flat and broad and peaks at z = 9.9 Å, 2 Å deeper than the lactone ring Å (Fig. S7B and Table S3). The rest of the molecule, arbitrarily named MHM, behaves the same as the overall molecule, even having the maximum of the PDC occurring at the same location as the whole molecule.

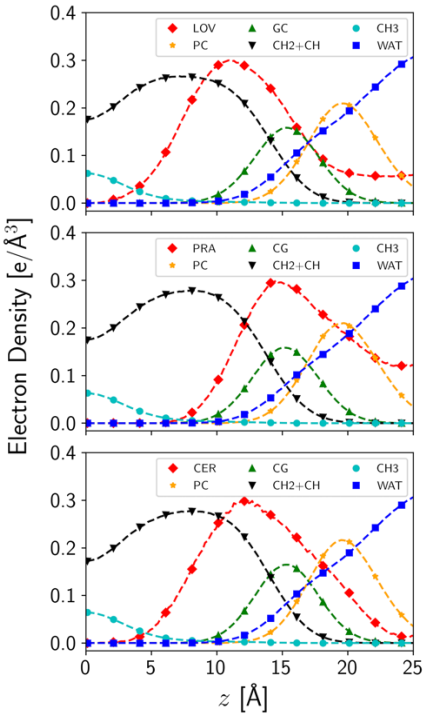

Fig. 4. EDPs of statins along the z axis of the POPC bilayer in the last 300 ns of the simulations.

To gain more insight into the localization of statins within the bilayer, we assessed the orientation of statins (Fig. 1) in the bilayer with respect to the bilayer's normal. The angle made by the pravastatin vector and the bilayer's normal fluctuated within a narrow range that was centered at 25˚ (Fig 5). The orientation of cerivastatin was similar to that pravastatin, with an angle that also fluctuated around 25˚ (Fig. 5). Unlike the charged statins, the neutral lovastatin showed a much wider range of angle fluctuation (Fig. 5).

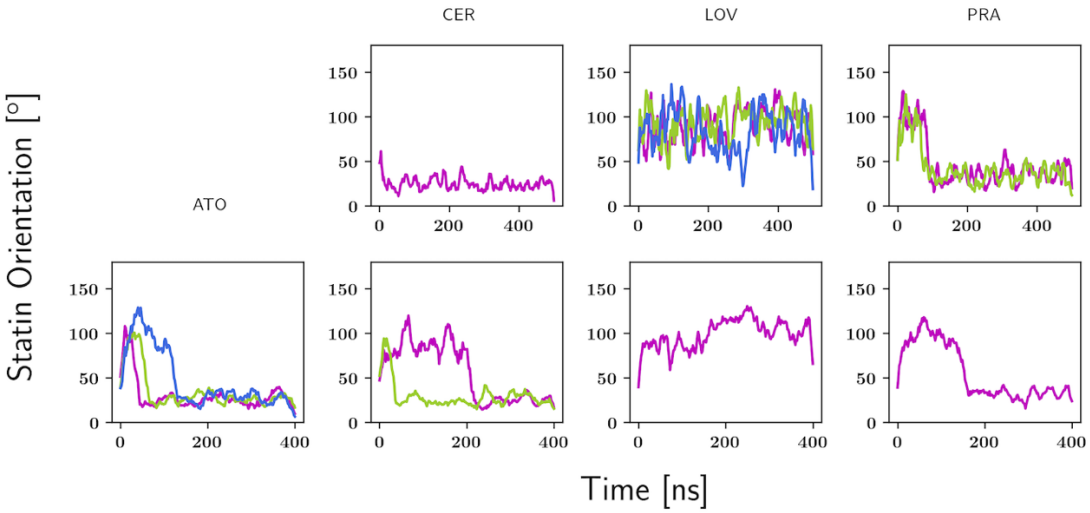

Fig. 5. The orientation of statin during the simulation. Only statins finally bound to the bilayers are plotted. Upper panel: the 20 mol% simulations, and each color represents a single statin molecule; lower panel: the titration simulations, and each color represents a replica. The orientation is measured by the angle between the director marked on Fig. 1 and the bilayer normal.

The thickness of the bilayer can be a great metric for comparing computational data to experiments. The thickness can also be used to assess the effect of different compounds and conditions on the membrane. The four statins had different effects on the thicknesses. As shown in Table 3, the statins decreased the thickness of the hydrophobic cores ($2D_C$) except for atorvastatin that never reached the hydrophobic core. The pure POPC had a 28.4 ± 0.1 Å $2D_C$, wider than the 27.5 ± 0.1 Å of pravastatin and the 27.8 ± 0.1 Å lovastatin and cerivastatin systems. The atorvastatin system had a $2D_C$ value of 28.3 ± 0.3 Å, not a significant difference from that of the pure POPC ($p = 0.58$) bilayer.

All statins systems had a decrease in both headgroup-to-headgroup distance (D_{HH}). The D_{HH} of the pure POPC was 39.1 ± 0.1 Å. All the statin systems had very similar D_{HH} values, all close to 37.9 Å. The pure POPC system had an overall bilayer thickness (D_B) of 38.0 ± 0.1 Å,

larger than all the statin systems. The D_B values of the statin systems were a little more spread out in comparison to the D_{HH} values. At 37.3 ± 0.3 Å, atorvastatin had a larger D_B than pravastatin, cerivastatin, and lovastatin, which had D_B values of 36.4 ± 0.1, 36.0 ± 0.6, and 35.7 ± 0.5 Å, respectively. Atorvastatin appears to interact strongly with the lipid headgroup to influence the thickness values in this region.

The thickness values can be used to roughly assess the degree of water penetration into the head group. Water penetration can be quantified as D_{HH} - D_B. A positive difference indicates water penetration into the headgroup while a negative difference indicates repulsion. All the systems had a positive difference, and the water penetration indicated by the thicknesses is confirmed by the great overlap between the water and PC PDCs across all the systems.

Table 3. Thicknesses (Å**)** of each system for different regions. D_{HH} is the head-to-head distance, D_B is the overall bilayer thickness, and $2D_C$ is the hydrophobic thickness.

	POPC	PRA	CER	ATO	LOV
$2D_C$ (Å)	28.4 ± 0.1	27.5 ± 0.1	27.8 ± 0.1	28.3 ± 0.2	27.8 ± 0.1
D_{HH} (Å)	39.1 ± 0.1	37.8 ± 0.2	37.9 ± 0.1	38.0 ± 0.4	37.7 ± 0.1
D_B (Å)	38.0 ± 0.1	36.4 ± 0.1	36.0 ± 0.6	37.3 ± 0.3	35.7 ± 0.3

4. Discussion

MD simulations conducted using all-atom force fields like CHARMM36 can be used to gain insight into the positioning of molecules in the membrane with high resolution. Galiulinna et al. were able to localize four statins, two of which, cerivastatin and atorvastatin, were also investigated in this work. Unfortunately, we did not observe binding of atorvastatin to the bilayer in the 20 mol% systems. Atorvastatin is a hydrophobic compound with an octanol-water partition coefficient log$P$ = 2.63[21], and it is expected that it would prefer the hydrophobic environment of the membrane over the aqueous solvent. Instead of binding to the membrane, atorvastatin formed large aggregates. Galiullina et al. showed that atorvastatin could bind to a phospholipid bilayer. We hypothesized that the lack of binding we observed was mainly caused by the aggregate formation, as demonstrated by the relatively wide COM RDFs between atorvastatin molecules (Fig. S2) and their increased values at short distances. The high concentration of the drugs was the main driving force for aggregates formation as demonstrated by the titration simulations using

only one drug molecule - binding of atorvastatin to the membrane occurred in all the three titration replicas (Fig. S1-b). Group-based RDFs between atorvastatin and POPC in the single-molecule simulations showed that the dihydroxy pentanoate of atorvastatin primarily interacted with the choline moiety of POPC, followed by the phosphate (Fig. S8). This is expected as the negatively charged pentanoate would be attracted to the positively charged choline and the polar solvent. The RDFs suggest that the more hydrophobic region of atorvastatin was localized deeper in the membrane. Even though atorvastatin did not bind to the membrane in the 20 mol% simulations, there were distant electrostatic interactions between the headgroup and the dihydroxy pentanoate (Fig. 2 and Fig. S7D). We expect that increasing the number of replicas and simulation duration would eventually allow for binding of atorvastatin to occur at the high concentration used by Galiullina and colleagues.

Cerivastatin on the other hand bound to the membrane within the first 150 ns of the simulation in one of the 20 mol% systems. Additionally, binding of cerivastatin to the membrane also occurred in all the three single-molecule simulation replicas. Cerivastatin has a slightly greater hydrophilicity than atorvastatin, log$P$ = 1.74[21]. In accordance with the experimental work by Galiullina et al. [21], the data we obtained from MD simulations suggest that cerivastatin aromatic rings mostly interact with the region of the bilayer just under the carbonyl and above the double bond of the acyl chains. The NMR data relied on the chemical shift induced by nearby aromatic rings for the localization of the statins, but this only provides a partial picture of the localization of the molecule. The EDPs obtained from the MD simulation reproducing the concentration used by Galiullina et al. suggest that different regions of cerivastatin interacts with different regions of the membrane. We used group-based RDFs between the different moieties of statins and POPC to get more details on the localization of cerivastatin. In accordance with EDPs, group-based RDFs show that the hydroxy pentanoate mostly interacts with the headgroup of POPC, more precisely the choline group. This is expected as the negatively charged pentanoate is attracted to the positive charge of the choline and would also interact favorably with the solvent. The RDFs also show that the distal isopropyl group of cerivastatin interacted less with the polar components of the membrane (the headgroup, glycerol, and carbonyl) in comparison to the pentanoate group and the fluorophenyl group. This is seen via a shift of RDF curves toward larger distances away from the polar POPC for the distal isopropyl in comparison to the in comparison to the pentanoate group and the fluorophenyl group. The RDFs and the EDPs suggest that cerivastatin has a particular

orientation in the membrane with the dihydroxy pentanoate interacting with the solvent, headgroup, and the glycerol, the fluorophenyl group in the middle interacting mostly with the atoms close to the second carbon of the acyl chain, the aromatic rings interacting with the methylene in the middle of the acyl chain, and the distal isopropyl group attached the pyridine ring goes deeper in the bilayer. This orientation is confirmed by a direct calculation of the molecule orientation over time. As shown in Fig. 5, the cerivastatin vector defined in Fig. 1 makes an angle with the bilayer normal that fluctuates around 25˚ after binding. This polarity is expected given the amphipathic character of cerivastatin. The data generated from the single-molecule simulations are similar to what we saw with 20 mol% simulations for cerivastatin.

Pravastatin is the most hydrophilic of all the statins investigated in this work with its octanol-water partition coefficient of log*P*=-0.56[21]. Galiullina et al. could not localize pravastatin in their POPC bilayer because of lack of resolution in the data[21]. In our simulations, pravastatin bound to the membrane well before the 100 ns mark. The data obtained from the MD simulations suggest that pravastatin, similarly to cerivastatin, tends to maintain a particular orientation while interacting with POPC. The EDPs show that the dihydroxy pentanoate group was mostly interacting with the phosphatidylcholine portion of POPC and the solvent. This is in accordance with the RDFs data, which show the polar and negatively charged dihydroxy pentanoate primarily interacting with the choline group. The EDPs suggest that the rings mostly interact with the region of POPC in between the *cis* double bond and the carbonyl. Pravastatin has a unique feature that differentiates from all the statins, and that is the presence of a hydroxyl group on one of its hydrophobic rings. The RDFs show that the hydroxyl group was closely interacting with the phosphate of POPC (Fig. S9). Further analysis of atom-atom RDFs indicates the hydroxyl group could potentially be an H-bond donor to the phosphate group and the carbonyl group (Fig. S10). The EDPs also show that the 1-methylpropyl attached to the ester localizes deeper in the bilayer than the rest of the molecule. With EDPs and RDFs, we can infer that the two rings are located right below the carbonyl with the ester and 1-methylpropyl groups protruding toward the hydrocarbon chains of POPC and the hydroxyl group protrudes toward the head group to interact with phosphate and the carbonyl via H-bond. The shape of the positional distribution curves of the hydroxyl, ester, and 1-methylpropyl groups from EDPs suggest pravastatin is mobile in the membrane while maintaining its orientation. This orientation is confirmed by the direct calculation of the angle between the pravastatin vector defined in Fig. 1 and the bilayer normal, which

fluctuated around 25˚ after binding. The fact that there is membrane binding for pravastatin systems may seem to contradict the negative log*P* value. However, there are a few important factors to keep in mind. The first fact is that Galiullina et al. experimentally observed binding of pravastatin to membranes. The second factor is that the higher hydrophilicity of pravastatin decreases aggregation and allows more single pravastatin molecules to diffuse to and interact with the membrane. Finally, Fig. S1-a and the EDPs show that pravastatin is mostly interacting with the hydrophilic portion of the membrane.

Lovastatin is another unique statin in that it is administered in its inactive lactone form. Galiullina et al. could not confidently establish the location of lovastatin in the POPC bilayer for the same reasons as pravastatin[21]. However, Shurshalova et al. could get the localization of lovastatin in micelles with both NMR and MD simulations[23]. In accordance with the data from Shurshalova et al.[23] and the high octanol-water partition coefficient (log*P* = 1.74) experimentally obtained by Galiullina et al.[21], our data suggest that lovastatin positions itself deep in the membrane, mostly interacting with the acyl chains and the carbonyl and glycerol regions of the membrane. The EPDs and RDFs suggest that lovastatin freely diffuses in the bilayer as its moieties interact similarly with the different parts of POPC. Furthermore, in addition to being localized deeper in the membrane, the EDPs and RDFs suggest that the tendency to maintain orientation after binding is weaker in lovastatin than in pravastatin and cerivastatin, and this is confirmed by the angle formed between the lovastatin vector (Fig. 1) and the bilayer normal fluctuating in a much wider range in comparison to cerivastatin and pravastatin (Fig. 5).

The data presented by Galiullina et al. show that statins can modulate many physical properties of the membrane[21]. The data we obtained from MD simulations also support the idea of differential modulation of the membrane by statins, but there are some caveats. In accordance with Galiullina et al., the data from our MD simulations show that statins decrease the chain order parameter of the palmitoyl's carbons overall. However, there are some discrepancies between the experimental data from Galiullina et al. and ours. For instance, lovastatin had the least effect on S_{CD} in the experiment by Galiullina et al.[21] while our data suggest the opposite. Furthermore, the overall reduction S_{CD} seen in the work Galiullina et al.[21] is larger than what we see in our data. A possible explanation is the short simulation time not allowing statins to reach their membrane/solution partition equilibrium and resulting in a small number of statins in the membrane. Fig. S11 in the supplementary document compares the S_{CD} obtained experimentally[21]

to that of our simulations. The fact that lovastatin appears to have a greater effect on S_{CD} than pravastatin and the other statins could be partially explained by the fact that the lovastatin system had the highest numbers of molecules that bound to the membrane during the simulations. The same can be said about the APL where we saw a direct relationship between the number of lipids in the membrane and the APL. The EDPs data suggest the thicknesses are also modulated by the statins, all causing reduction of $2D_C$, D_{HH}, and $D_{B.}$ The decrease of D_{HH} and $D_{B.}$ can be explained by the close interactions of statins and the headgroups of the bilayer, as shown in the EDPs. The lack of modulation of $2D_C$ in the atorvastatin systems suggests that statins influence the $2D_C$ only if close interaction occurs.

Although POPC is the most abundant phospholipid in mammalian plasma membrane (PM) and endoplasmic reticulum (ER)[51], the use of a POPC-only bilayer has limitations. A major limitation is the absence of cholesterol in the membrane models as statins can potentially have additional/different effects on the membrane in the presence of cholesterol. This could be important since statins share a similar structure with cholesterol and can interact with it within the membrane. Nevertheless, the pure POPC model is adequate to estimate the location of statin within the membrane given its abundance in biological membranes. Future works will utilize more realistic membrane composition after getting data from simple membranes. The goal of this work was to see if we can obtain data comparable to that of the NMRs experiment and use it as a foundation to perform further simulations on bilayers more representative of that of the PM and ER in terms of lipid composition.

The discrepancies between the experimental data from Galiullina et al. and ours could originate from the formation of aggregates that prevented more statins from binding to the membrane. We hypothesized that the high concentration of statins in solution facilitated the aggregation and thereby reduced the number of free statin molecules available to diffuse to the membrane and interact with it. This greatly reduces the potential influence of statins on the physical characteristics of the membrane and prevents us from seeing the significant decrease in order parameter that Galiullina et al. saw. Nevertheless, we are still able to see that statins can reduce the order parameter of phospholipid membranes and the location of statins within those membranes. As previously noted, we ran additional titration simulations (three replicas for each statin) with only one statin molecule per system instead of twenty per system. In accordance with our hypothesis, the binding of drugs to the membrane increased, as all the twelve single-molecule

systems showed binding in comparison to only five for the twenty-molecules systems. The localization within the bilayer and the interaction with the membrane were similar between the single- molecule systems and the twenty-molecule systems across all the statins.

5. Conclusion

Statins are a class of efficacious cholesterol-lowering drugs that competitively inhibit the synthesis of cholesterol. Both clinical and in vitro experiments have revealed numerous pleiotropic effects of statins. Statins have different pleiotropic effects, and the current evidence motivates the hypothesis that these cholesterol-independent effects of statins depend on their localization in the membrane. Our study aimed to gain some insight into the localization of atorvastatin, cerivastatin, lovastatin, and pravastatin within a POPC bilayer. The data we obtained from the MD simulation suggest that lovastatin is localized deep in the membrane and has more flexibility in orientation while pravastatin is localized closer to the bilayer/solvent interface and maintains a certain range of orientations, driven by the interaction of its polar dihydroxy group with both the solvent and the head groups of the bilayer. Cerivastatin is closer to lovastatin than pravastatin in its localization, but it still maintains the similar orientation trend seen in pravastatin, albeit with much less interaction with the solvent. We did not observe atorvastatin binding to the membrane in the 20 mol% simulations, but the titration simulations indicated it adopting a certain orientation once bound to the membrane with the dihydroxy pentanoate located at the membrane-water interface while the hydrophobic part located deeper in the bilayer. In addition to the localization within the membrane, we also looked at the effect of statins on the membrane. The data show a decrease in S_{CD} and an increase in APL by all the statins that bound the membrane. The data also show a decrease in D_{HH} and D_B by all the statins. However, the effects of statins on the membrane structure are predicted to heavily depend on the adsorption level of the statins. The data obtained with the POPC bilayer model will be useful in the development of simulations that will utilize membrane models with more accurate lipid composition. An example of a modification for future works would be the inhibition of self-aggregation by slowly titrating the statins as they bind to the membrane instead of introducing all the statins at once. Reducing self-aggregation may lead to more statins binding to the membrane and thereby portraying a more accurate representation of the interaction of statins with biological membranes.

6. Supporting Material Available

Figures for drug location (*z*-axis); statin COM RDF; APL over time; palmitoyl chain carbons S_{CD} combined; oleyl chain carbons S_{CD}; EDPs for pure POPC, atorvastatin, component of cerivastatin, lovastatin, and pravastatin; group-based RDFs between statin and POPC; atom-atom RDFs between PRA and POPC. Table for statin binding; peaks of positional distribution curves of cerivastatin, lovastatin, and pravastatin's components; peaks of positional distribution curves of POPC's components for each system. The stream file and penalty scores for each statin.

7. Acknowledgements

This research is in part by supported by the NSF (MCB-1951425 and CHE-2003912) and the NIH intramural program (YY). We would like to acknowledge our computational support from the University of Maryland's Deeptought2 which is maintained by the Division of Information Technology and a joint UMD/JHU computational resource MARCC.

8. References

1. Lozano, R.; Naghavi, M.; Foreman, K.; Lim, S.; Shibuya, K.; Aboyans, V.; Abraham, J.; Adair, T.; Aggarwal, R.; Ahn, S. Y., Global and regional mortality from 235 causes of death for 20 age groups in 1990 and 2010: a systematic analysis for the Global Burden of Disease Study 2010. *The lancet* **2012,** *380* (9859), 2095-2128.
2. Fuentes, A. V.; Pineda, M. D.; Venkata, K. C. N., Comprehension of top 200 prescribed drugs in the US as a resource for pharmacy teaching, training and practice. *Pharmacy* **2018,** *6* (2), 43-43.
3. Solberg, L. A.; Strong, J. P., Risk factors and atherosclerotic lesions. A review of autopsy studies. *Arteriosclerosis: An Official Journal of the American Heart Association, Inc.* **1983,** *3* (3), 187-198.
4. Grundy, S. M., Cholesterol and coronary heart disease: a new era. *Jama* **1986,** *256* (20), 2849-2858.
5. LaRosa, J. C.; Hunninghake, D.; Bush, D.; Criqui, M. H.; Getz, G. S.; Gotto Jr, A. M.; Grundy, S. M.; Rakita, L.; Robertson, R. M.; Weisfeldt, M. L., The cholesterol facts. A summary of the evidence relating dietary fats, serum cholesterol, and coronary heart disease. A joint statement by the American Heart Association and the National Heart, Lung, and Blood Institute. The Task Force on Cholesterol Iss. *Circulation* **1990,** *81* (5), 1721-1733.

6. Shekelle, R. B.; Shryock, A. M.; Paul, O.; Lepper, M.; Stamler, J.; Liu, S.; Raynor Jr, W. J., Diet, serum cholesterol, and death from coronary heart disease: the Western Electric Study. *New England Journal of Medicine* **1981,** *304* (2), 65-70.
7. Stancu, C.; Sima, A., Statins: mechanism of action and effects. *Journal of cellular and molecular medicine* **2001,** *5* (4), 378-387.
8. Maron, D. J.; Fazio, S.; Linton, M. F., Current perspectives on statins. *Circulation* **2000,** *101* (2), 207-213.
9. Liao, J. K.; Laufs, U., Pleiotropic effects of statins. *Annu. Rev. Pharmacol. Toxicol.* **2005,** *45*, 89-118.
10. Athyros, V. G.; Kakafika, A. I.; Tziomalos, K.; Karagiannis, A.; Mikhailidis, D. P., Pleiotropic effects of statins-clinical evidence. *Current pharmaceutical design* **2009,** *15* (5), 479-489.
11. Blum, A.; Shamburek, R., The pleiotropic effects of statins on endothelial function, vascular inflammation, immunomodulation and thrombogenesis. *Atherosclerosis* **2009,** *203* (2), 325-330.
12. Bonnet, J.; McPherson, R.; Tedgui, A.; Simoneau, D.; Nozza, A.; Martineau, P.; Davignon, J.; Investigators, C. A. P., Comparative effects of 10-mg versus 80-mg Atorvastatin on high-sensitivity C-reactive protein in patients with stable coronary artery disease: results of the CAP (Comparative Atorvastatin Pleiotropic effects) study. *Clinical therapeutics* **2008,** *30* (12), 2298-2313.
13. Plenge, J. K.; Hernandez, T. L.; Weil, K. M.; Poirier, P.; Grunwald, G. K.; Marcovina, S. M.; Eckel, R. H., Simvastatin lowers C-reactive protein within 14 days: an effect independent of low-density lipoprotein cholesterol reduction. *Circulation* **2002,** *106* (12), 1447-1452.
14. Srinivasa Rao, K.; Prasad, T.; Mohanta, G. P.; Manna, P. K., An overview of statins as hypolipidemic drugs. *IJPSDR* **2011,** *3* (3), 178-183.
15. Schachter, M., Chemical, pharmacokinetic and pharmacodynamic properties of statins: an update. *Fundamental & clinical pharmacology* **2005,** *19* (1), 117-125.
16. Mason, R. P.; Walter, M. F.; Day, C. A.; Jacob, R. F., Intermolecular differences of 3-hydroxy-3-methylglutaryl coenzyme a reductase inhibitors contribute to distinct pharmacologic and pleiotropic actions. *The American journal of cardiology* **2005,** *96* (5), 11-23.
17. Imran, T. F.; Wong, A.; Schneeweiss, S.; Desai, R., Hydrophilic Statins Are Associated With a Lower Risk of Incident Heart Failure Than Lipophilic Statins in a Large National Database. *Circulation* **2017,** *136* (suppl_1), A17590-A17590.
18. Corsini, A., The safety of HMG-CoA reductase inhibitors in special populations at high cardiovascular risk. *Cardiovascular drugs and therapy* **2003,** *17* (3), 265-285.
19. Larocque, G.; Arnold, A. A.; Chartrand, É.; Mouget, Y.; Marcotte, I., Effect of sodium bicarbonate as a pharmaceutical formulation excipient on the interaction of fluvastatin with membrane phospholipids. *European Biophysics Journal* **2010,** *39* (12), 1637-1647.
20. Mason, R. P., Molecular basis of differences among statins and a comparison with antioxidant vitamins. *The American journal of cardiology* **2006,** *98* (11), S34-S41.
21. Galiullina, L. F.; Scheidt, H. A.; Huster, D.; Aganov, A.; Klochkov, V., Interaction of statins with phospholipid bilayers studied by solid-state NMR spectroscopy. *Biochimica et Biophysica Acta (BBA)-Biomembranes* **2019,** *1861* (3), 584-593.
22. Bellosta, S.; Paoletti, R.; Corsini, A., Safety of statins: focus on clinical pharmacokinetics and drug interactions. *Circulation* **2004,** *109* (23_suppl_1), III-50.

23. Shurshalova, G. S.; Yulmetov, A. R.; Sharapova, D. A.; Aganov, A. V.; Klochkov, V. V., Interaction of Lovastatin with Model Membranes by NMR Data and from MD Simulations. *BioNanoScience* **2020**, 1-9.
24. Moradi, S.; Nowroozi, A.; Shahlaei, M., Shedding light on the structural properties of lipid bilayers using molecular dynamics simulation: a review study. *RSC advances* **2019,** *9* (8), 4644-4658.
25. Klauda, J. B., Perspective: Computational modeling of accurate cellular membranes with molecular resolution. *The Journal of Chemical Physics* **2018,** *149* (22), 220901-220901.
26. Smiatek, J.; Oprzeska-Zingrebe, E. A., Some Notes on the Thermodynamic Accuracy of Coarse-Grained Models. *Frontiers in molecular biosciences* **2019,** *6*, 87-87.
27. Pignatello, R.; Musumeci, T.; Basile, L.; Carbone, C.; Puglisi, G., Biomembrane models and drug-biomembrane interaction studies: Involvement in drug design and development. *Journal of pharmacy and bioallied sciences* **2011,** *3* (1), 4-4.
28. Leonard, A. N.; Wang, E.; Monje-Galvan, V.; Klauda, J. B., Developing and testing of lipid force fields with applications to modeling cellular membranes. *Chemical reviews* **2019,** *119* (9), 6227-6269.
29. Jo, S.; Kim, T.; Iyer, V. G.; Im, W., CHARMM-GUI: A web-based graphical user interface for CHARMM. *Journal of Computational Chemistry* **2008,** *29* (11), 1859-1865.
30. Jo, S.; Kim, T.; Im, W., Automated builder and database of protein/membrane complexes for molecular dynamics simulations. *PLoS ONE* **2007,** *2* (9).
31. Wu, E. L.; Cheng, X.; Jo, S.; Rui, H.; Song, K. C.; Dávila-Contreras, E. M.; Qi, Y.; Lee, J.; Monje-Galvan, V.; Venable, R. M.; Klauda, J. B.; Im, W., CHARMM-GUI membrane builder toward realistic biological membrane simulations. John Wiley and Sons Inc.: 2014; Vol. 35, pp 1997-2004.
32. Phillips, J. C.; Braun, R.; Wang, W.; Gumbart, J.; Tajkhorshid, E.; Villa, E.; Chipot, C.; Skeel, R. D.; Kale, L.; Schulten, K., Scalable molecular dynamics with NAMD. *Journal of computational chemistry* **2005,** *26* (16), 1781-1802.
33. Kim, S.; Lee, J.; Jo, S.; Brooks, C. L.; Lee, H. S.; Im, W., CHARMM-GUI ligand reader and modeler for CHARMM force field generation of small molecules. *Journal of Computational Chemistry* **2017,** *38* (21), 1879-1886.
34. Vanommeslaeghe, K.; Hatcher, E.; Acharya, C.; Kundu, S.; Zhong, S.; Shim, J.; Darian, E.; Guvench, O.; Lopes, P.; Vorobyov, I.; Mackerell, A. D., CHARMM general force field: A force field for drug-like molecules compatible with the CHARMM all-atom additive biological force fields. *Journal of Computational Chemistry* **2010,** *31* (4), 671-690.
35. Vanommeslaeghe, K.; MacKerell, A. D., Automation of the CHARMM general force field (CGenFF) I: Bond perception and atom typing. *Journal of Chemical Information and Modeling* **2012,** *52* (12), 3144-3154.
36. Vanommeslaeghe, K.; Raman, E. P.; MacKerell, A. D., Automation of the CHARMM General Force Field (CGenFF) II: Assignment of Bonded Parameters and Partial Atomic Charges. *Journal of Chemical Information and Modeling* **2012,** *52* (12), 3155-3168.
37. Yu, W.; He, X.; Vanommeslaeghe, K.; MacKerell, A. D., Extension of the CHARMM general force field to sulfonyl-containing compounds and its utility in biomolecular simulations. *Journal of Computational Chemistry* **2012,** *33* (31), 2451-2468.
38. Soteras Gutiérrez, I.; Lin, F. Y.; Vanommeslaeghe, K.; Lemkul, J. A.; Armacost, K. A.; Brooks, C. L.; MacKerell, A. D., Parametrization of halogen bonds in the CHARMM

general force field: Improved treatment of ligand–protein interactions. *Bioorganic and Medicinal Chemistry* **2016,** *24* (20), 4812-4825.
39. Brooks, B. R.; Brooks, C. L.; Mackerell, A. D.; Nilsson, L.; Petrella, R. J.; Roux, B.; Won, Y.; Archontis, G.; Bartels, C.; Boresch, S.; Caflisch, A.; Caves, L.; Cui, Q.; Dinner, A. R.; Feig, M.; Fischer, S.; Gao, J.; Hodoscek, M.; Im, W.; Kuczera, K.; Lazaridis, T.; Ma, J.; Ovchinnikov, V.; Paci, E.; Pastor, R. W.; Post, C. B.; Pu, J. Z.; Schaefer, M.; Tidor, B.; Venable, R. M.; Woodcock, H. L.; Wu, X.; Yang, W.; York, D. M.; Karplus, M., CHARMM: The biomolecular simulation program. *J. Comput. Chem.* **2009,** *30* (10), 1545-1614.
40. Klauda, J. B.; Venable, R. M.; Freites, J. A.; O'Connor, J. W.; Tobias, D. J.; Mondragon-Ramirez, C.; Vorobyov, I.; MacKerell Jr, A. D.; Pastor, R. W., Update of the CHARMM all-atom additive force field for lipids: validation on six lipid types. *The journal of physical chemistry B* **2010,** *114* (23), 7830-7843.
41. Jorgensen, W. L.; Chandrasekhar, J.; Madura, J. D.; Impey, R. W.; Klein, M. L., Comparison of simple potential functions for simulating liquid water. *The Journal of chemical physics* **1983,** *79* (2), 926-935.
42. Durell, S. R.; Brooks, B. R.; Ben-Naim, A., Solvent-induced forces between two hydrophilic groups. *The Journal of Physical Chemistry* **1994,** *98* (8), 2198-2202.
43. Feller, S. E.; Zhang, Y.; Pastor, R. W.; Brooks, B. R., Constant pressure molecular dynamics simulation: the Langevin piston method. *The Journal of chemical physics* **1995,** *103* (11), 4613-4621.
44. Martyna, G. J.; Tobias, D. J.; Klein, M. L., Constant pressure molecular dynamics algorithms. *The Journal of chemical physics* **1994,** *101* (5), 4177-4189.
45. Steinbach, P. J.; Brooks, B. R., New spherical-cutoff methods for long-range forces in macromolecular simulation. *Journal of computational chemistry* **1994,** *15* (7), 667-683.
46. Andersen, H. C., Rattle: A "velocity" version of the shake algorithm for molecular dynamics calculations. *Journal of Computational Physics* **1983,** *52* (1), 24-34.
47. Humphrey, W.; Dalke, A.; Schulten, K., VMD: visual molecular dynamics. *Journal of molecular graphics* **1996,** *14* (1), 33-38.
48. Chodera, J. D., A Simple Method for Automated Equilibration Detection in Molecular Simulations. *J. Chem. Theory Comput.* **2016,** *12* (4), 1799-1805.
49. Nagle, J. F., Area/lipid of bilayers from NMR. *Biophys. J.* **1993,** *64* (5), 1476-1481.
50. Boughter, C. T.; Monje-Galvan, V.; Im, W.; Klauda, J. B., Influence of Cholesterol on Phospholipid Bilayer Structure and Dynamics. *J. Phys. Chem. B* **2016,** *120* (45), 11761-11772.
51. van Meer, G.; Voelker, D. R.; Feigenson, G. W., Membrane lipids: where they are and how they behave. *Nature Reviews Molecular Cell Biology* **2008,** *9* (2), 112-124.